NeuroImage 49 (2010) 1–8

Contents lists available at ScienceDirect

NeuroImage

journal homepage: www.elsevier.com/locate/ynimg

Combining shape and connectivity analysis: An MRI study of thalamic degeneration in Alzheimer's disease

Mojtaba Zarei [a,c,*,1], Brian Patenaude [a,1], Jessica Damoiseaux [b], Ciro Morgese [a], Steve Smith [a], Paul M. Matthews [c], Frederik Barkhof [d], Serge Rombouts [e], Ernesto Sanz-Arigita [d], Mark Jenkinson [a]

[a] FMRIB Centre, John Radcliffe Hospital, Oxford OX3 9DU, UK
[b] Department of Neurology, University of Stanford, USA
[c] Imperial College London, Department of Clinical Neuroscience, London, UK
[d] Department of Radiology, VU University Medical Center, Amsterdam, Netherlands
[e] Leiden University Medical Centre, Leiden, Netherlands

ARTICLE INFO

Article history:
Received 16 April 2009
Revised 18 August 2009
Accepted 1 September 2009
Available online 8 September 2009

Keywords:
Alzheimer's disease
Thalamus
DTI
MRI
Shape analysis

ABSTRACT

Alzheimer's disease (AD) is associated with neuronal loss not only in the hippocampus and amygdala but also in the thalamus. Anterodorsal, centromedial, and pulvinar nuclei are the main sites of degeneration in AD. Here we combined shape analysis and diffusion tensor imaging (DTI) tractography to study degeneration in AD in the thalamus and its connections.

Structural and diffusion tensor MRI scans were obtained from 16 AD patients and 22 demographically similar healthy volunteers. The thalamus, hippocampus, and amygdala were automatically segmented using our locally developed algorithm, and group comparisons were carried out for each surface vertex. We also employed probabilistic diffusion tractography to obtain connectivity measures between individual thalamic voxels and hippocampus/amygdala voxels and to segment the internal medullary lamina (IML).

Shape analysis showed significant bilateral regional atrophy in the dorsal–medial part of the thalamus in AD patients compared to controls. Probabilistic tractography demonstrated that these regions are mainly connected with the hippocampus, temporal, and prefrontal cortex. Intrathalamic FA comparisons showed reductions in the anterodorsal region of thalamus. Intrathalamic tractography from this region revealed that the IML was significantly smaller in AD patients than in controls. We suggest that these changes can be attributed to the degeneration of the anterodorsal and intralaminar nuclei, respectively. In addition, based on previous neuropathological reports, ventral and dorsal–medial shape change in the thalamus in AD patients is likely to be driven by IML atrophy. This combined shape and connectivity analysis provides MRI evidence of regional thalamic degeneration in AD.

Introduction

Alzheimer's disease (AD) is the most common cause of dementia. Neuropathological hallmarks of AD are neurofibrillary tangles, β-amyloid plaques, as well as neuronal and synaptic loss (Braak and Braak, 1991b; Mirra et al., 1991). These pathological findings occur initially and predominantly in the medial temporal lobe structures including hippocampus and amygdala (Braak and Braak, 1991a,b). Hippocampal and, to a lesser extent, amydgalar atrophy in Alzheimer's disease have been well documented, whereas thalamic degeneration, particularly in the early stages of the disease, is controversial (Braak and Braak, 1991a; Paskavitz et al., 1995; Xuereb et al., 1991).

The thalamus is an important part of the Papez circuit. The hippocampus connects directly with the anterior thalamus via the fornix and to the pulvinar via the temporopulvinar tract. The hippocampus also indirectly connects with the anterior thalamus via the mammillary bodies. Integrity of these connections is essential for episodic memory (Aggleton and Brown, 1999), which is specifically impaired in Alzheimer's disease (Di Paola et al., 2007). In addition, some intralaminar nuclei, namely central medial, central lateral, and parafascicular nuclei, located within the internal medullar lamina (IML) were found to be involved at the early stages of AD (Rub et al., 2002; Xuereb et al., 1991). For this reason, we investigated the pattern of thalamic degeneration and its relation to the degeneration of the hippocampus and amygdala using a combination of structural MRI and diffusion tensor image analysis.

Analysis of the shape of subcortical structures provides useful information about the location and pattern of structural changes in neurological and psychiatric disorders. Using this method, several reports showed that CA1 is the primary site of degeneration of the

* Corresponding author. Fax: +44 1865 222717.
E-mail address: mojtaba@fmrib.ox.ac.uk (M. Zarei).
[1] These authors contributed equally.

1053-8119/$ – see front matter © 2009 Elsevier Inc. All rights reserved.
doi:10.1016/j.neuroimage.2009.09.001

hippocampus in AD (Qiu et al., 2008; Xu et al., 2008). Similar analyses have been done on the thalami of patients with schizophrenia (Coscia et al., 2009; Harms et al., 2007; Kang et al., 2008), obsessive–compulsive disorders (Kang et al., 2008), Parkinson's disease (McKeown et al., 2008) and Tourette's syndrome (Wang et al., 2007). Although there is only indirect evidence of regional thalamic atrophy in AD using shape analysis of cerebral ventricles (Ferrarini et al., 2008), postmortem pathological studies showed degeneration of pulvinar, intralaminar nuclei, and dorsolateral nuclei of the thalamus in AD (Xuereb et al., 1991). In addition, we have recently showed changes in the fractional anisotropy of white matter tracts in the proximity of the hippocampal formation in the temporal lobe using diffusion tensor imaging (Damoiseaux et al., 2008). An important feature of these tracts is the abundant connections between the medial temporal structures and the thalamus. Taken together, these findings provide a solid justification to use a combination of shape analysis and diffusion tensor tractography to study the pattern of degeneration of the thalamus in AD.

Method

Subjects

All data were obtained at the Alzheimer Center of the VU University Medical Centre, Amsterdam, the Netherlands. Our cohort included AD patients ($n=16$) and healthy elderly controls (EC, $n=22$), matched for age and sex. Diagnostic criteria of mild AD were that of NINCDS–ADRDA (McKhann et al., 1984), with MMSE scores greater than 18 and CDR less than 2. Healthy subjects were recruited by two means: (1) asking family members of patients and (2) advertisements posted in the medical centre, the medical faculty of the university and activity centres for the elderly in the community. The Medical Ethics Committee of the VU University Medical Centre Amsterdam approved the study. Written consent was obtained from all subjects or their legal guardian if necessary. Participants were excluded if they had any significant medical, neurological (except for the disease under study here in the patient group) or psychiatric illness; a history of brain damage; or if they were taking medication known to influence cerebral function (except for disease-related medication in the patient group). T2-weighted fluid attenuation inversion recovery (FLAIR) scans of each subject were reviewed by a neuroradiologist (F.B.) to assess vascular lesions using the Fazekas scale (Fazekas et al., 2002).

MRI acquisition

Magnetic resonance imaging (MRI) examinations were conducted on a 1.5 T Sonata system (Sonata, Siemens AG, Erlangen, Germany), and included a heavily T1-weighted 3D gradient sequence (TR = 2700 ms; TI = 450 ms; TE = 3.97 ms; flip angle = 8°, 160 coronal slices; voxel size = 1 × 1.5 × 1 mm). DTI was measured using an echo planar imaging (EPI) sequence (Reese et al., 2003) with the following specifications: TR = 8500 ms, TE = 86 ms, voxel size: 2 mm isotropic, 59 consecutive slices, acquisition matrix = 128 mm × 128 mm (FOV = 256 mm), 6/8 partial Fourier, 60 diffusion directions with b-value = 700 s/mm^2, and 10 images with no diffusion weighting ($b=0$ s/mm^2). The bandwidth was 1860 Hz/pixel. Head motion was minimized by the use of tightly padded clamps attached to the head coil.

Image analysis

Image analysis was carried out using tools from FSL (FMRIB Software Library, http://www.fmrib.ox.ac.uk/fsl)(Smith et al., 2004). BET was used for brain extraction of the T1-weighted images and FLIRT was used to perform affine alignment of the diffusion and T1-weighted images. Effects of eddy currents and head motion were reduced by registering all the diffusion-weighted images to a non-diffusion-weighted reference image using an affine, 12 degrees of freedom registration. Analyses of the diffusion images were carried out using tools from FDT (FMRIB Diffusion Toolkit). Probabilistic modelling of diffusion parameters and tractography were carried out using previously described methods (Behrens et al., 2007). The FIRST tool (part of FSL) was used to automatically segment subcortical grey matter structures, including the hippocampus, amygdala and thalamus (Patenaude et al., 2007). The results of each step of the image processing, including subcortical segmentation, were carefully examined by a neuroscientist (M.Z.) to ensure accuracy of the results. The diagram below shows how combined DTI and structural image analysis contributed to this study.

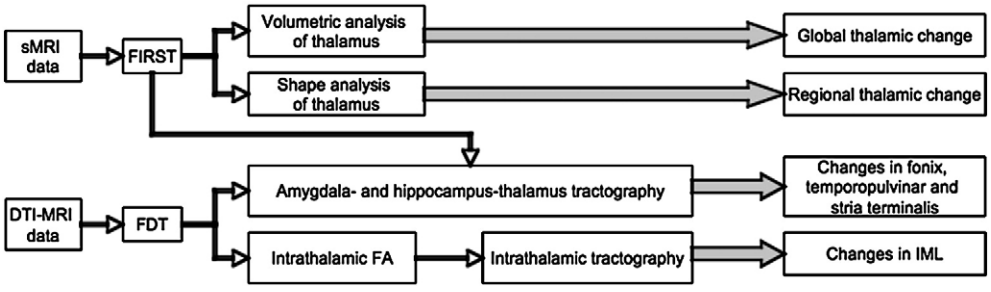

FIRST is a probabilistic adaptation of the active appearance model (Cootes and Taylor, 2004). The method is informed by the shape and intensity variations of a structure from a training set for the purpose of automatically segmenting the structure. A multivariate Gaussian model of vertex location and intensity variation is used, and is based on having point correspondence across subjects (same number and labelling of vertices across subjects). The necessary correspondence is imposed during the parameterization of the labelled images with a deformable model. The model is fit to new images by maximising the posterior probability of shape given the observed intensities.

Statistical analyses

Demographic and neuropsychological data

Demographic variables were compared between groups. Age, education and neuropsychological test scores (i.e., MMSE) were compared using Student's t-tests (2-tailed, $p<0.05$).

Volumetric group comparison

Volumes of the subcortical structures were normalized for differences in total intracranial volume among subjects by means

of an analysis of covariance approach (ANOVA), using coefficients obtained from the control group (Jack et al., 1989). Region-of-interest (ROI) volumes were compared between patients with AD and normal control subjects using a general linear model (GLM) multiple regression analysis with sex, age and education as covariates (MANCOVA). Left and right ROIs were analysed separately. If the overall models were found to be significantly different between groups, differences in individual regions were assessed. Omnibus tests were two-tailed with alpha set at 0.05, and effect size of the overall model calculated using η^2. Corrections for multiple comparisons of post-hoc tests were carried out using Bonferroni correction.

Vertex analysis

FIRST creates a surface mesh for each subcortical structure using a deformable mesh model. The mesh is composed of a set of triangles and the apex of adjoining triangles is called a vertex. The number of vertices for each structure is fixed so that corresponding vertices can be compared across individuals and between groups. Vertex correspondence is crucial for the FIRST methodology, as it facilitates the investigation of localized shape differences through the examination of group differences in the spatial location of each vertex. Although the vertices retain correspondence, the surfaces reside in the native image space, and thus have an arbitrary orientation/position. Therefore, the surfaces must all be aligned to a common space prior to investigating any group differences. The mean surface from the FIRST models (in MNI152 space) is used as the target to which surfaces from the individual subjects are aligned. Pose (rotation and translation) is removed by minimizing the sum-of-squares difference between the corresponding vertices of a subject's surface and the mean surface (target). Group comparisons of vertices were carried out using *F*-statistics (Patenaude et al., 2007).

Diffusion tensor imaging analysis

Unconstrained probabilistic tractography was used to assess connectivity between seed and target(s) using the FMRIB diffusion tool (Behrens et al., 2007). We carried out three tractography analyses. Firstly, voxels within the thalamus were classified according to the probability of their connectivity to the hippocampus and amygdala separately. Clusters of voxels were thresholded at 25% of the maximum probability of connectivity to their target. This allowed us to identify areas of the thalamus that are most likely to be connected to either the hippocampus or the amygdala. Secondly, we carried out tractography between the hippocampus/amygdala (seeds), and the thalamus (target) to visualize their anatomical connections. Thirdly, we subtracted the group fractional anisotropy (FA) maps of the thalamus in MNI space for the AD group from that of the elderly controls, in order to identify the focus of the maximum change within the thalamus. A similar comparison was done using the mean diffusivity (MD). To assess whether between-group differences in FA and MD were significant, we used tract-based spatial statistics (Smith et al., 2006) only within the interior of the thalamus. Finally, for the segmentation of the internal medullary lamina (IML) we identified the voxel that had the highest between-group FA difference and used that as the seed to carry out tractography within the thalamus. The resulting voxels were thresholded at 25% of the maximum connectivity strength. Mean FA value and volume of the IML were compared between groups using a MANCOVA.

Neuropsychological correlations

We studied possible correlations between neuropsychological measures and mean FA values, within the tracts/regions of interest. The mean FA values were extracted from FA maps that were registered into native structural space. Group comparisons were done using an ANOVA. The patient characteristics and neuropsychological measures that were included in the correlation analyses were those that differed significantly between groups. Correlation analyses were performed using Spearman's rho one-tailed tests, corrected for multiple comparisons ($p<0.01$).

Table 1
Demographic data (mean ± SEM).

	EC	AD
Sex (M/F ratio)	9/13	8/8
Age (years)	70.7 ± 6.0	69.5 ± 6.7
Handedness (EHI)	9.7 ± 0.9	9.9 ± 0.3
Education (years)	14.7 ± 3.2	14.4 ± 3.1
Cigarettes (per week)	9.6 ± 22.1	0.0 ± 0.0
Alcoholic beverages per week (units)	9.2 ± 8.8	9.3 ± 11.1
Premorbid IQ (NART – Dutch version)	110.7 ± 18.7	102.5 ± 19.7
Fazekas score	0.0 ± 0.0	0.88 ± 0.88
Mini mental state examination score*	28.7 ± 1.4	22.9 ± 3.2

Demographic data of the cohort show that AD and control subjects had similar characteristics and only differed significantly in their cognitive function (*$p<0.0001$ with independent *t*-tests).
NART = National Adult Reading Test.

Results

Demographic data

The two groups had similar characteristics with no significant differences in mean age, sex, or education (Table 1). Predictably, cognitive status, as assessed by neuropsychological tests, was significantly decreased in the patients with AD compared with normal control subjects. The degree of vascular loading was comparable between groups, with mostly punctiform white matter lesions in both groups. No focal lacunar infarcts were identified in the thalamus.

Table 2
Neuropsychological profile of each group (mean ± SEM).

	AD	EC
15 word test, delayed recall*	1.6 ± 0.4	8.4 ± 0.7
15 word test, total direct recall*	21.9 ± 1.5	42.9 ± 2.3
Digit span backward	3.9 ± 0.3	5.1 ± 0.2
Digit span forward	5.0 ± 0.4	6.2 ± 0.2
Fluency insects (1 min)*	4.7 ± 0.6	8.9 ± 0.7
Fluency, 2 min*	18.3 ± 1.7	35.2 ± 1.7
Maze mistakes	4.6 ± 1.2	2.2 ± 0.3
Maze total time	299 ± 42	204 ± 14
Memory impairment scale, delayed recall	2.8 ± 0.7	10.6 ± 0.3
Memory impairment scale, direct recall*	8.8 ± 0.6	11.1 ± 0.2
Rey complex figure, copy	25.9 ± 2.9	32.7 ± 0.7
Rey complex figure, organization	1.9 ± 0.5	3.3 ± 0.4
Score TMTB divided by score TMTA	3.6 ± 0.3	2.4 ± 0.2
Stroop color	84.7 ± 6.5	60.8 ± 2.3
Stroop color–word	180.3 ± 18.8	121.9 ± 6.3
Stroop word	54.7 ± 3.4	46.2 ± 1.4
Trail making test A	72.2 ± 7.5	43.55 ± 3.29
Trail making test B	251.4 ± 35.9	95.1 ± 7.6
Visual association test A (1 + 2)*	5.12 ± 0.9	11.50 ± 0.2
Visual association test B (1 + 2)	3.1 ± 0.9	9.2 ± 0.8
WAIS symbol substitution	36.8 ± 5.5	58.7 ± 3.3
WAIS symbol substitution, implicit learning associations*	2.5 ± 0.8	9.4 ± 0.9
WAIS symbol substitution, implicit learning free recall*	3.1 ± 0.4	6.4 ± 0.3

Neuropsychological profiles of each group shows that the AD group had significant recall, delayed memory, fluency, visual association, and implicit memory differences when compared with normal control (*$p<0.005$, corrected for multiple comparisons with age, gender, and level of education as covariants; MANCOVA).
WAIS = Weschler Adult Intelligence Scale, TMT = trail making test A and B.

Table 3
Volumetric data of ROIs; mean ± SEM (mm^3).

		AD	EC
Left hemisphere	Stria terminalis	934 ± 144	902 ± 83
	Amygdala*	1319 ± 83	1519 ± 80
	Fornix	982 ± 108	10,283 ± 9112
	Hippocampus*	3059 ± 118	3715 ± 107
	IML*	211 ± 30	393 ± 38
	Thalamus*	7742 ± 207	7981 ± 202
Right hemisphere	Stria terminalis	858 ± 82	1078 ± 113
	Amygdala*	1376 ± 103	1591 ± 70
	Fornix	1080 ± 111	7262 ± 6035
	Hippocampus*	3246 ± 164	3806 ± 139
	IML	338 ± 57	387 ± 33
	Thalamus*	7634 ± 221	8073 ± 199

Comparison of the volumes of the regions of interest showed significant reduction of the volume of the amygdala, hippocampus, and thalamus bilaterally, as well as the left internal medullary lamina (IML) in the AD patients compared with the control group (*$p<0.005$ corrected for multiple comparisons, with age and gender as covariants; MANCOVA).

Neuropsychology

AD patients performed worse than healthy control subjects on the MMSE, digit span, 15 word test, WAIS symbol substitution, delayed recall of memory impairment scale, fluency, and trail making test B (Table 2).

Quantitative volumetric data

The results of group comparisons of the ROI volumes are shown in Table 3. This table shows that the amygdala, hippocampus, and thalamus were all smaller in AD patients compared to control subjects in both hemispheres. In addition, the volume of the fornix in both hemispheres, was much smaller in AD patients than in the control group, which is consistent with previous observations (Copenhaver et al., 2006). However, this difference failed to reach statistical significance in the between-group comparison due the wide intersubject variability. The left IML was significantly smaller in the AD subjects compared to the control subjects.

Linear regression of the volumes of the ROIs showed that the strongest correlate of thalamic and hippocampal atrophy in each hemisphere was the volume of the thalamus ($R^2 = 0.78$, $B = 0.775$, $p<0.0001$) and the hippocampus ($R^2 = 0.79$, $B = 0.562$, $p<0.0001$), respectively, in the contralateral hemisphere. In another regression, using FA values, the mean FA of fornix was the best "predictor" of the volume of these tracts and of the FA of IMLs.

Shape analysis using vertex-based comparisons

Comparisons of vertex locations between AD and control groups showed significant regional atrophy (inward movement of vertices in the AD subjects) bilaterally on the dorsal–medial and ventral aspects of thalamus. In the left thalamus, two patches of shrinkage were seen, one located at the posterior end and one at the anterior end (Fig. 1A). A small patch was also seen on the ventral aspect of the left thalamus. In the right thalamus, patches of shrinkage were seen at the anterior end in the dorsal and ventral aspects for the AD subjects (Fig. 1A). Spatial comparison of these changes with the Oxford Thalamic Connectivity Probability Atlas (Behrens et al., 2003) showed that these regions mainly corresponded with the areas of the thalamus that are connected with the temporal cortex and the prefrontal cortex (Fig. 1B).

DTI tractography

Tractography between the hippocampus/amygdala and thalamus showed clear connections between these structures. DTI tractography showed that the hippocampus connects to the anterior thalamus via

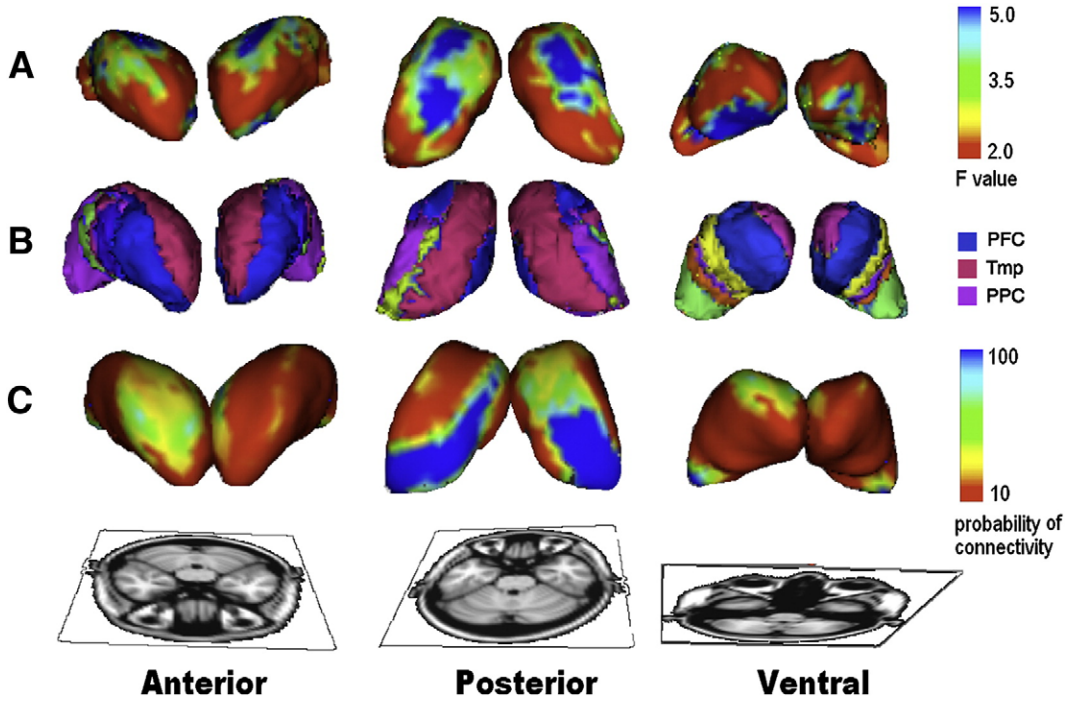

Fig. 1. (A) Vertex-wise comparison of the thalamus between healthy subjects and AD patients shows focal atrophy on the dorsal and ventral aspects of thalamus. (B) The Oxford Thalamic Connectivity Probability Atlas shows that the dorsal–medial aspect of the thalamus is connected to the temporal cortex (red) and the ventral anterior part of the prefrontal cortex (blue). (C) Voxel-wise tractography between the thalamus and the hippocampus shows maximum connectivity on the dorsal-posterior aspect of the thalamus. Comparing A, B, and C shows that the majority of the shape changes correspond to regions that are connected with the temporal cortex, hippocampus, and prefrontal cortex. The bottom row illustrates the angle at which the thalamus is being viewed. For vertex-wise shape analysis (A) *F*-statistics have degrees of freedom of 3,34 giving $p = 0.13$ ($F = 2$), $p = 0.1$ ($F = 2.25$), $p = 0.03$ ($F = 3.5$), and $p = 0.006$ ($F = 5$). For tractography (C), the color-coded bar represents the connectivity strength.

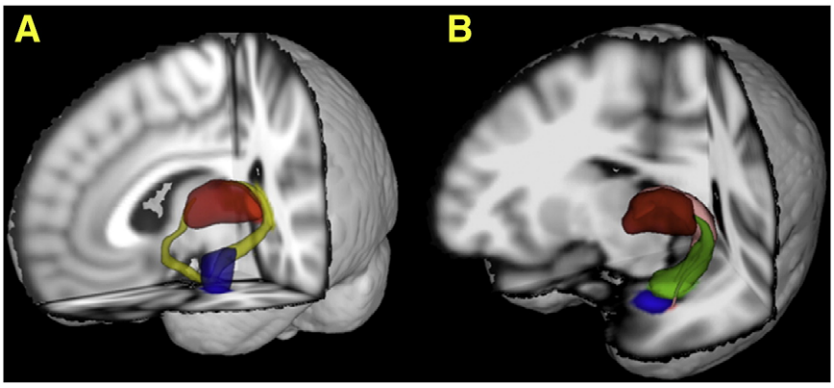

Fig. 2. Probabilistic tractography shows (A) amygdalar connections with the anterior thalamus via the fornix and uncinate faciculus, as well as hippocampal connections (B) with the anterior thalamus via the fornix, and with the pulvinar via the temporopulvinar tract. These images are created using probabilistic tractography between the amygdala and the thalamus, or the hippocampus and the thalamus in the healthy controls and are thresholded to include at least 70% of the cases. Note that these images do not aim to show the details of the anatomy. For example, the mammillary bodies, the mammillothalamic tracts, the corticohypothalamic tract, and the subiculothalamic tract are not shown (amygdala = blue, hippocampus = green, thalamus = red, fornix and temporopulvinar tracts = pink, and ventral amygdalofugal pathway = yellow).

the fornix and to the pulvinar via the temporopulvinar tract (Fig. 2). Indirect hippocampal fornical connection to the anterior thalamus through the mammillary body was not investigated. The fornix and temporopulvinar tracts approach the thalamus from the posterior and dorsal aspect of the thalamus. The amygdala connects with the anterior thalamus through the stria terminalis, whose course is almost in parallel with the fornix. The segmentation of these tracts was based on DTI tractography between the amygdala and the thalamus (stria terminalis) and the hippocampus and the thalamus (fornix). We differentiated these tracts from each other based on the probability of connectivity of the voxels to the amygdala or the hippocampus, as well as by visual inspection. The amygdala also connects with the dorsomedial nucleus of the thalamus via the amygdalofugal pathways that run medially and rostrally (Fig. 2).

Classification of the surface voxels of the thalamus according to their connectivity with the hippocampus and the amygdala showed that voxels connected to the hippocampus and/or the amygdala are located on the dorsal–medial portion of the thalamus (Fig. 1). These correspond to posterior vertices that showed significant changes in their spatial location in the shape analysis group comparison.

Quantitative DTI

Comparing FA within the thalamus between the groups showed that the maximal reduction in FA is found in the dorsal–anterior region of thalamus (Fig. 3A). Similarly, maximum mean diffusivity (MD) measures were noted in this area. We carried out intrathalamic tractography from the voxel that showed the maximum FA reduction in the AD group and this showed an entire intrathalamic tract that anatomically corresponds with the internal medullary lamina (Fig. 3B). Visual comparison of the result of shape analysis of the thalamus with the IML shows spatial correspondence between the IML atrophy and surface changes in the ventral and dorsal–medial thalamic regions.

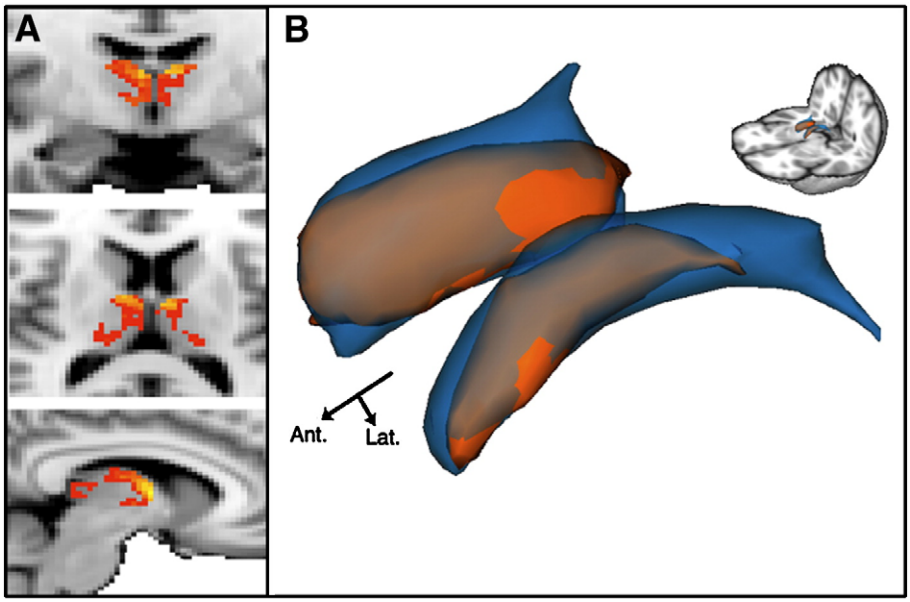

Fig. 3. (A) Voxel-wise FA analysis within the thalamus shows decreased mean FA within the internal medullary lamina for the AD patients compared with control subjects. The maximum reduction of FA occurs in the anterodorsal nucleus of the thalamus, which is the focus of thalamic degeneration in AD. (B) Internal medullary lamina can be visualized using probabilistic tractography. The IML volume is smaller in the AD patients (red) than in the controls (blue) ($p<0.001$ for the left hemisphere). Note that in our AD population, hippocampal atrophy was more severe in the left hemisphere than in the right. Comparing this image with the shape analysis in Fig. 1 shows that the IML is located beneath the regional atrophy that is seen on the surface of the thalamus using vertex analysis.

Table 4
Quantitative DTI data.

			AD	EC
Fractional anisotropy	Left	Amygdala	0.168 ± 0.004	0.173 ± 0.010
		Hippocampus	0.146 ± 0.003	0.163 ± 0.011
		IML	0.247 ± 0.010	0.256 ± 0.011
		Stria terminalis	0.283 ± 0.007	0.297 ± 0.011
		Fornix	0.227 ± 0.010	0.248 ± 0.008
		Thalamus**	0.287 ± 0.008	0.333 ± 0.006
	Right	Amygdala*	0.18 ± 0.008	0.205 ± 0.008
		Hippocampus	0.149 ± 0.005	0.153 ± 0.006
		IML**	0.274 ± 0.010	0.305 ± 0.007
		Stria terminalis*	0.281 ± 0.006	0.326 ± 0.016
		Fornix**	0.222 ± 0.010	0.257 ± 0.009
		Thalamus*	0.3328 ± 0.00479	0.36 ± 0.00994
Mean diffusivity	Left	Amygdala	0.0011 ± 0.0001	0.0012 ± 0.0001
		Hippocampus*	0.0016 ± 0.0001	0.0014 ± 0.0001
		Stria terminalis	0.0013 ± 0.0001	0.0012 ± 0.0001
		Fornix	0.0019 ± 0.0001	0.0016 ± 0.0001
		Thalamus	0.0019 ± 0.0002	0.0018 ± 0.0001
	Right	Stria terminalis*	0.0014 ± 0.0001	0.0011 ± 0.0001
		Amygdala	0.0012 ± 0.0001	0.0011 ± 0.00004
		Hippocampus**	0.0015 ± 0.0001	0.0013 ± 0.00004
		Fornix	0.0017 ± 0.0001	0.0015 ± 0.0001
		Thalamus	0.0019 ± 0.0002	0.0016 ± 0.0001

Comparison of FA measures for the ROIs shows reduction of FA in the thalami, right amygdala, amygdalar tract, hippocampal tract, and internal medullary lamina in the AD group when compared to the control group. There is also an increase in MD in the hippocampi and right amygdala in the AD group compared to the control group (**$p<0.001$, *$p<0.05$; MANCOVA).

Group comparison of mean FA showed a significant reduction of FA in the right thalamus, amygdala, stria terminalis, fornix, and IML in AD patients (Table 4). The left thalamus showed an increased mean FA in AD patients. Comparison of MD between groups showed an increase in the left fornix, right stria terminalis, and right hippocampus in AD patients (Table 4).

Neuropsychological correlates of the ROIs

To investigate the relationship between the MRI markers and neuropsychological impairments, we carried out linear regression with a stepwise method (Table 5). We found that left hippocampal atrophy is the best predictor for all neuropsychological deficits except trail making test B and verbal fluency (insects) (Table 5).

This analysis showed that episodic memory correlates strongly and consistently with the volume of hippocampi and left IML, as well as FA in the right IML. Delayed recall correlated with the volume of hippocampi, left IML, right thalamus, right amygdala, and FA in the right IML. The volumes of the thalami, left hippocampus, and left IML consistently correlated with tests of executive function, particularly the trail making test B. The Rey complex figure tests showed no correlation with any of the markers.

Discussion

This study explores the pattern of thalamic degeneration in AD. For the first time we used a combination of shape and connectivity-based analyses on structural and DTI data sets, respectively. We successfully identified regional thalamic atrophy in AD that can be attributed to degenerative changes in the hippocampal-thalamic network. More specifically, we identified surrogate imaging markers that relate to the degeneration of anterodorsal nucleus of thalamus, pulvinar, and intralaminar nuclei in AD, consistent with previously reported postmortem studies (Xuereb et al., 1991).

Comparing the volumes of the thalamus between groups demonstrated that this structure undergoes significant atrophy in early AD. Vertex analysis provided further insight into the nature of this atrophy, which is characterised by a depression (inward movement of vertices in the AD group) in the dorsal–medial and ventral aspect of the thalamus bilaterally. The tractography-based analysis showed that dorsal–medial atrophy of the thalamus corresponds to changes in connectivity with the anterior temporal cortex and the posterior hippocampus. The hippocampus is the primary site of neuronal degeneration in AD (Braak et al., 2006) and has direct connections with the anterior thalamus via the fornix and indirect connections via mammillary bodies through the mammillothalamic tract (Shipley, 1974). There is also a non-fornical connection between the hippocampus and the pulvinar part of thalamus via the temporopulvinar tract. We also visualized the stria terminalis that connects the amygdala with the anterior thalamic nuclei as well as the ventral amygdalofugal pathway, which connects the amygdala with the dorsomedial and intralaminar nuclei of the thalamus.

Table 5
Linear regression of neuropsychological measures with imaging markers.

	Model predictors	Dependent variable	R^2	F	p	β	t
Volume	Left hippocampus	MMSE	0.2	12.7	0.001	0.5	3.6
	Left hippocampus	Backwards digit span	0.2	8.55	0.006	0.4	2.9
	Left hippocampus	Forwards digit span	0.2	8.55	0.006	0.4	2.9
	Left hippocampus	15 word test, direct recall	0.3	17.9	0.0001	0.6	4.2
	Left hippocampus	15 word test, delayed recall	0.3	17.1	0.0001	0.6	4.1
	Left hippocampus + Right amygdala	Implicit learning – free recall	0.5	14.3	0.0001	0.5	4.3
	Left hippocampus	Implicit learning associations	0.3	16.6	0.0001	0.6	4.1
	Left hippocampus	Delayed recall	0.5	30.6	0.0001	0.7	5.5
	Left hippocampus + Left IML	Verbal fluency	0.3	9.3	0.001	0.3	2.1
	Left IML + right amygdala	Verbal fluency – insects	0.3	9.0	0.001	0.4	2.4
	Left IML	Trail making test B	0.2	108	0.002	−0.5	−3.8
FA	Right IML + Left fornix	MMSE	0.9	1186	<0.001	0.7	2.8
	Right IML	Forward digit span	0.9	707	<0.001	0.9	26.6
	Right IML	Backwards digit span	0.9	684	<0.001	0.9	26.1
	Right IML	15 word test, direct recall	0.9	295	<0.001	0.9	17.1
	Right fornix + Left stria terminalis	15 word test, delayed recall	0.7	52	<0.001	−1.1	−2.5
	Right fornix	Association	0.7	73	<0.001	0.8	8.5
	Right IML	Free recall	0.8	257	<0.001	0.9	16.1
	Right fornix	Delayed recall	0.8	148	<0.001	0.9	12.2
	Right IML	Fluency	0.9	329	<0.001	0.9	18.1
	Right IML	Fluency – insect	0.8	189	<0.001	0.9	13.7
	Right IML	Trail making test B	0.6	53	<0.001	−0.7	−7.3

Shows the relationship between the neuropsychological measures and the MRI markers using linear regression with a stepwise method.

Postmortem studies suggested that the anterodorsal nucleus is the primary site of degeneration in the thalamus of AD patients (Braak and Braak, 1991a; Xuereb et al., 1991). These studies showed at least 80% cell loss in this nucleus in AD patients (Xuereb et al., 1991). We suggested that reductions of FA in the anterodorsal part of thalamus are likely to be due to degeneration of the anterodorsal nucleus. Since this area is located in the anterior part of the IML, the FA change, in part, reflects pathological changes in the mammillothalamic tract. Strong correlations of neuropsychological measures of episodic memory with the volumes of left hippocampus and IML may be due to a combination of degeneration of the anterodorsal nucleus, the mammillary tract, and the hippocampus.

It is unlikely that FA change in the anterior thalamic region is related to changes in the anteroventral or anteromedial nuclei, as postmortem studies established that these nuclei do not degenerate in AD (Xuereb et al 1991). In addition to hippocampal connections, the anterodorsal nucleus has substantial connections with the retrosplenial limbic area while the anteroventral and lateral dorsal nuclei are principally connected with the cingulate area proper (Kaitz and Robertson, 1981; Robertson and Kaitz, 1981). Interestingly, postmortem studies show that the severity of neurofibrillary tangles and cell loss is greater in the retrosplenial area than in the posterior cingulate cortex, and that the anterior cingulate gyrus is relatively spared until late in AD (Brun and Englund, 1981). Disruption of this circuit causes severe impairment of episodic memory in animals and humans (Aggleton and Brown, 1999; Aggleton et al., 1996; Kumral et al., 2001; Sener et al., 1993).

Although degeneration of the anterodorsal nucleus may functionally contribute to the symptomatology of AD, it is unlikely to be the cause of the shape changes in the thalamus that we found using vertex-based analysis. This is due to the fact that the anterodorsal nucleus is a thin layer of cells curving around the anteroventral nucleus and therefore is only a small portion of the entire thalamic volume. However, intrathalamic tractography used to visualize the IML, shows it contains efferents and afferents of thalamic nuclei as well as intralaminar nuclei. Spatial correspondence between the IML and the surface depression of the thalamus suggests that the regional shape change could be due to IML degeneration. The IML was markedly smaller in the left hemisphere of AD patients, which corresponds well with the more severe atrophy seen in the left hippocampus of this AD population. Strong correlation of the volume of the hippocampus and the volume of the IML further supports this notion. Interestingly, the posterior portion of the IML appears to be more atrophied than the anterior portion. The posterior IML contains fibers that mainly connect the posterior parietal, precuneus, cuneus, and posterior cingulate to the pulvinar (Brun and Englund, 1981; Hunt et al., 2007). It also contains centromedial and centrolateral nuclei that were shown to degenerate considerably in AD (Xuereb et al., 1991).

DTI tractography revealed a non-fornical connection between the hippocampus and thalamus. This connection originates from the entorhinal cortex, subiculum, presubiculum, and parasubiculum and terminates in the pulvinar via the temporopulvinar tract (Saunders et al., 2005). The pulvinar, in turn, has rich connections with the posterior parietal cortex and the precuneus, which are also pathological targets in AD (Brun and Englund, 1981; Hunt et al., 2007). Postmortem studies showed neuronal loss in the pulvinar in AD (Kuljis, 1994; Leuba and Saini, 1995; Xuereb et al., 1991). Some of the cognitive symptoms in AD, such as spatial–visual impairment and visual hallucinations, may be attributed to the pathology of this region and connected structures. This notion is further supported by fMRI studies showing decreased reactivity in the precuneus in patients with dementia (Rombouts et al., 2007).

We propose that the early degeneration of structures that are anatomically and functionally directly connected (i.e., the hippocampus, anterodorsal nucleus, pulvinar, retrospenial cingulate, and precuneus) may indicate that the pattern of degeneration is mainly driven by the connectivity. We propose that the distribution of cellular and subcellular changes seen in neurodegenerative disorders, at least partly, depends on the connectivity of the structures involved. It is hypothesised that specific homeostatic mechanisms, and the number, strength, and architecture of connections within a network could account for phenomena such as the formation, organization and degeneration in the neuronal circuits (Wilson et al., 2007). Some neurobiological studies support this hypothesis. For example, the dopamine signalling pathway was shown to play an important role in the survival of target neurons in the striatum (Tang et al., 2007). Further neurobiological, as well as modelling studies are required to test this hypothesis.

Study limitations

A combination of shape and DTI analyses can be useful in the study of neurodegenerative disorders; however, the approach requires further testing to assess its consistency and reproducibility. In addition, the measures used are not direct surrogate markers of degeneration of the subthalamic nuclei but can be related to them. Knowledge of anatomical pathology is essential in relating markers to the pathological process, although the ultimate proof can only be provided by pathological validation of these markers.

Conclusion

This study shows that a combination of DTI and shape analyses can be useful to identifying converging evidence of degeneration of the thalamus in patients with Alzheimer's disease. Similar approaches might be useful in the study of subcortical structures in other neurodegenerative disorders.

Acknowledgments

This study was supported by the Institute for the Study of Aging (ISOA grant number: 231002), the Netherlands Organization for Scientific Research (NWO grant number: 916.36.117), the UK BBSRC (M.J.) and the UK Department of Health (M.Z.), and EPSRC (B.P.).

References

Aggleton, J.P., Brown, M.W., 1999. Episodic memory, amnesia, and the hippocampal–anterior thalamic axis. Behav. Brain Sci. 22, 425–444 discussion 444-489.
Aggleton, J.P., Hunt, P.R., Nagle, S., Neave, N., 1996. The effects of selective lesions within the anterior thalamic nuclei on spatial memory in the rat. Behav. Brain Res. 81, 189–198.
Behrens, T.E., Berg, H.J., Jbabdi, S., Rushworth, M.F., Woolrich, M.W., 2007. Probabilistic diffusion tractography with multiple fibre orientations: what can we gain? NeuroImage 34, 144–155.
Behrens, T.E.J., Johansen-Berg, H., Woolrich, M.W., Smith, S.M., Wheeler-Kingshott, C.A.M., Boulby, P.A., Barker, G.J., Sillery, E.L., Sheehan, K., Ciccarelli, O., Thompson, A.J., Brady, J.M., Matthews, P.M., 2003. Non-invasive mapping of connections between human thalamus and cortex using diffusion imaging. Nat. Neurosci. 6, 750–757.
Braak, H., Alafuzoff, I., Arzberger, T., Kretzschmar, H., Del Tredici, K., 2006. Staging of Alzheimer disease-associated neurofibrillary pathology using paraffin sections and immunocytochemistry. Acta Neuropathol. 112, 389–404.
Braak, H., Braak, E., 1991a. Alzheimer's disease affects limbic nuclei of the thalamus. Acta. Neuropathol. 81, 261–268.
Braak, H., Braak, E., 1991b. Neuropathological stageing of Alzheimer-related changes. Acta. Neuropathol. (Berl) 82, 239–259.
Brun, A., Englund, E., 1981. Regional pattern of degeneration in Alzheimer's disease: neuronal loss and histopathological grading. Histopathology 5, 549–564.
Cootes, T.F., Taylor, C.J., 2004. Anatomical statistical models and their role in feature extraction. Br. J. Radiol. 77 (Spec No 2), S133–139.
Copenhaver, B.R., Rabin, L.A., Saykin, A.J., Roth, R.M., Wishart, H.A., Flashman, L.A., Santulli, R.B., McHugh, T.L., Mamourian, A.C., 2006. The fornix and mammillary bodies in older adults with Alzheimer's disease, mild cognitive impairment, and cognitive complaints: a volumetric MRI study. Psychiatry Res. 147, 93–103.
Coscia, D.M., Narr, K.L., Robinson, D.G., Hamilton, L.S., Sevy, S., Burdick, K.E., Gunduz-Bruce, H., McCormack, J., Bilder, R.M., Szeszko, P.R., 2009. Volumetric and shape

analysis of the thalamus in first-episode schizophrenia. Hum. Brain Mapp. 30, 1236–1245.
Damoiseaux, J.S., Smith, S.M., Witter, M.P., Arigita, E.J., Barkhof, F., Scheltens, P., Stam, C.J., Zarei, M., Rombouts, S.A., 2008. White matter tract integrity in aging and Alzheimer's disease. Hum. Brain Mapp. 30, 1051–1059.
Di Paola, M., Macaluso, E., Carlesimo, G.A., Tomaiuolo, F., Worsley, K.J., Fadda, L., Caltagirone, C., 2007. Episodic memory impairment in patients with Alzheimer's disease is correlated with entorhinal cortex atrophy. A voxel-based morphometry study. J. Neurol. 254, 774–781.
Fazekas, F., Ropele, S., Schmidt, R., 2002. Can small-vessel disease-related cerebral abnormalities be used as a surrogate marker for vascular dementia trials? J. Neural. Transm. Suppl. 61–67.
Ferrarini, L., Palm, W.M., Olofsen, H., van der Landen, R., Jan Blauw, G., Westendorp, R.G., Bollen, E.L., Middelkoop, H.A., Reiber, J.H., van Buchem, M.A., Admiraal-Behloul, F., 2008. MMSE scores correlate with local ventricular enlargement in the spectrum from cognitively normal to Alzheimer disease. NeuroImage 39, 1832–1838.
Harms, M.P., Wang, L., Mamah, D., Barch, D.M., Thompson, P.A., Csernansky, J.G., 2007. Thalamic shape abnormalities in individuals with schizophrenia and their nonpsychotic siblings. J. Neurosci. 27, 13835–13842.
Hunt, A., Schönknecht, P., Henze, M., Seidl, U., Haberkorn, U., Schröder, J., 2007. Reduced cerebral glucose metabolism in patients at risk for Alzheimer's disease. Psychiatry Res. 155, 147–154.
Jack Jr., C.R., Twomey, C.K., Zinsmeister, A.R., Sharbrough, F.W., Petersen, R.C., Cascino, G.D., 1989. Anterior temporal lobes and hippocampal formations: normative volumetric measurements from MR images in young adults. Radiology 172, 549–554.
Kaitz, S.S., Robertson, R.T., 1981. Thalamic connections with limbic cortex: II. Corticothalamic projections. J. Comp. Neurol. 195, 527–545.
Kang, D.H., Kim, S.H., Kim, C.W., Choi, J.S., Jang, J.H., Jung, M.H., Lee, J.M., Kim, S.I., Kwon, J.S., 2008. Thalamus surface shape deformity in obsessive–compulsive disorder and schizophrenia. NeuroReport 19, 609–613.
Kuljis, R.O., 1994. Lesions in the pulvinar in patients with Alzheimer's disease. J. Neuropathol. Exp. Neurol. 53, 202–211.
Kumral, E., Evyapan, D., Balkir, K., Kutluhan, S., 2001. Bilateral thalamic infarction. Clinical, etiological and MRI correlates. Acta. Neurol. Scand. 103, 35–42.
Leuba, G., Saini, K., 1995. Pathology of subcortical visual centres in relation to cortical degeneration in Alzheimer's disease. Neuropathol. Appl. Neurobiol. 21, 410–422.
McKeown, M.J., Uthama, A., Abugharbieh, R., Palmer, S., Lewis, M., Huang, X., 2008. Shape (but not volume) changes in the thalami in Parkinson disease. BMC Neurol. 8, 8.
McKhann, G., Drachman, D., Folstein, M., 1984. Clinical diagnosis of Alzheimer's disease: Report of the NINCDS–ADRDA work group under the auspices of Department of Health and Human Services Task Force on Alzheimer's disease. Neurology 34, 939–944.
Mirra, S.S., Heyman, A., McKeel, D., Sumi, S.M., Crain, B.J., Brownlee, L.M., Vogel, F.S., Hughes, J.P., Van Belle, G., Berg, L., 1991. The Consortium to Establish a Registry for Alzheimer's Disease (CERAD). Part II. Standardization of the neuropathologic assessment of Alzheimer's disease. Neurology 41, 479–486.
Paskavitz, J.F., Lippa, C.F., Hamos, J.E., Pulaski-Salo, D., Drachman, D.A., 1995. Role of the dorsomedial nucleus of the thalamus in Alzheimer's disease. J. Geriatr. Psychiatry Neurol. 8, 32–37.
Patenaude, B., Smith, S., Kennedy, D., Jenkinson, M., 1989. FMRIB Technical Report TR07BP1. Oxford, Bayesian Shape and Appearance Models, pp. 1–23.
Qiu, A., Younes, L., Miller, M.I., Csernansky, J.G., 2008. Parallel transport in diffeomorphisms distinguishes the time-dependent pattern of hippocampal surface deformation due to healthy aging and the dementia of the Alzheimer's type. NeuroImage 40, 68–76.
Reese, T.G., Heid, O., Weisskoff, R.M., Wedeen, V.J., 2003. Reduction of eddy-current-induced distortion in diffusion MRI using a twice-refocused spin echo. Magn. Reson. Med. 49, 177–182.
Robertson, R.T., Kaitz, S.S., 1981. Thalamic connections with limbic cortex: I. Thalamocortical projections. J. Comp. Neurol. 195, 501–525.
Rombouts, S.A., Damoiseaux, J.S., Goekoop, R., Barkhof, F., Scheltens, P., Smith, S.M., Beckmann, C.F., 2007. Model-free group analysis shows altered BOLD FMRI networks in dementia. Hum. Brain Mapp. 30, 256–266.
Rub, U., Del Tredici, K., Del Turco, D., Braak, H., 2002. The intralaminar nuclei assigned to the medial pain system and other components of this system are early and progressively affected by the Alzheimer's disease-related cytoskeletal pathology. J. Chem. Neuroanat. 23, 279–290.
Saunders, R.C., Mishkin, M., Aggleton, J.P., 2005. Projections from the entorhinal cortex, perirhinal cortex, presubiculum, and parasubiculum to the medial thalamus in macaque monkeys: identifying different pathways using disconnection techniques. Exp. Brain Res. 167, 1–16.
Sener, R.N., Alper, H., Yunten, N., Dundar, C., 1993. Bilateral acute thalamic infarcts causing thalamic dementia. AJR Am. J. Roentgenol. 161, 678–679.
Shipley, M.T., 1974. Presubiculum afferents to the entorhinal area and the Papez circuit. Brain Res. 67, 162–168.
Smith, S.M., Jenkinson, M., Woolrich, M.W., Beckmann, C.F., Behrens, T.E., Johansen-Berg, H., Bannister, P.R., De Luca, M., Drobnjak, I., Flitney, D.E., Niazy, R.K., Saunders, J., Vickers, J., Zhang, Y., De Stefano, N., Brady, J.M., Matthews, P.M., 2004. Advances in functional and structural MR image analysis and implementation as FSL. NeuroImage 23 (Suppl. 1), S208–219.
Smith, S.M., Jenkinson, M., Johansen-Berg, H., Rueckert, D., Nichols, T.E., Mackay, C.E., Watkins, K.E., Ciccarelli, O., Cader, M.Z., Matthews, P.M., Behrens, T.E., 2006. Tract-based spatial statistics: voxelwise analysis of multi-subject diffusion data. NeuroImage 31, 1487–1505.
Tang, T.S., Chen, X., Liu, J., Bezprozvanny, I., 2007. Dopaminergic signaling and striatal neurodegeneration in Huntington's disease. J. Neurosci. 27, 7899–7910.
Wang, L., Lee, D.Y., Bailey, E., Hartlein, J.M., Gado, M.H., Miller, M.I., Black, K.J., 2007. Validity of large-deformation high dimensional brain mapping of the basal ganglia in adults with Tourette syndrome. Psychiatry Res. 154, 181–190.
Wilson, N.R., Ty, M.T., Ingber, D.E., Sur, M., Liu, G., 2007. Synaptic reorganization in scaled networks of controlled size. J. Neurosci. 27, 13581–13589.
Xu, Y., Valentino, D.J., Scher, A.I., Dinov, I., White, L.R., Thompson, P.M., Launer, L.J., Toga, A.W., 2008. Age effects on hippocampal structural changes in old men: the HAAS. NeuroImage 40, 1003–1015.
Xuereb, J.H., Perry, R.H., Candy, J.M., Perry, E.K., Marshall, E., Bonham, J.R., 1991. Nerve cell loss in the thalamus in Alzheimer's disease and Parkinson's disease. Brain 114 (Pt. 3), 1363–1379.

Update

NeuroImage
Volume 51, Issue 2, June 2010, Page 940

DOI: https://doi.org/10.1016/j.neuroimage.2010.03.019

NeuroImage 51 (2010) 940

Contents lists available at ScienceDirect

NeuroImage

journal homepage: www.elsevier.com/locate/ynimg

Corrigendum

Corrigendum to "Combining shape and connectivity analysis: An MRI study of thalamic degeneration in Alzheimer's disease" [NeuroImage 49 (2010) 1–8]

Mojtaba Zarei [a,c,*,1], Brian Patenaude [a,1], Jessica Damoiseaux [b], Ciro Morgese [a], Steve Smith [a], Paul M. Matthews [c], Frederik Barkhof [d], S.A.R.B. Rombouts [e], Ernesto Sanz-Arigita [d], Mark Jenkinson [a]

[a] FMRIB Centre, John Radcliffe Hospital, Oxford OX3 9DU, UK
[b] Department of Neurology, University of Stanford, USA
[c] Imperial College London, Department of Clinical Neuroscience, London, UK
[d] Department of Radiology, VU University Medical Center, Amsterdam, Netherlands
[e] Leiden Institute for Brain and Cognition, Institute for Psychological Research, and Department of Radiology, Leiden University Medical Center, Leiden, The Netherlands

Professor Serge Rombouts' name and his affiliations were incompletely mentioned in the author line in error. The correct author line is shown above.

DOI of original article: 10.1016/j.neuroimage.2009.09.001.
* Corresponding author. Imperial College London, Department of Clinical Neuroscience, London, UK. Fax: +44 1865 222717.
E-mail address: mojtaba@fmrib.ox.ac.uk (M. Zarei).
[1] These authors contributed equally.

doi:10.1016/j.neuroimage.2010.03.019